Adiabatic perturbation theory of electronic stopping in insulators

Andrew P. Horsfield*
Department of Materials and Thomas Young Centre, Imperial College London, London SW7 2AZ, United Kingdom

Anthony Lim and W. M. C. Foulkes
Department of Physics and Thomas Young Centre, Imperial College London, London SW7 2AZ, United Kingdom

Alfredo A. Correa
Lawrence Livermore National Laboratory, 7000 East Avenue, Livermore, California 94550, USA
(Received 12 April 2016; revised manuscript received 12 May 2016; published 2 June 2016)

A model able to explain the complicated structure of electronic stopping at low velocities in insulating materials is presented. It is shown to be in good agreement with results obtained from time-dependent density-functional theory for the stopping of a channeling Si atom in a Si crystal. If we define the repeat frequency $f = v/\lambda$, where λ is the periodic repeat length of the crystal along the direction the channeling atom is traveling, and v is the velocity of the channeling atom, we find that electrons experience a perturbing force that varies in time at integer multiples l of f. This enables electronic excitations at low atom velocity, but their contributions diminish rapidly with increasing values of l. The expressions for stopping power are derived using adiabatic perturbation theory for many-electron systems, and they are then specialized to the case of independent electrons. A simple model for the nonadiabatic matrix elements is described, along with the procedure for determining its parameters.

DOI: 10.1103/PhysRevB.93.245106

I. INTRODUCTION

There are several situations in which electronic devices are subject to impacts from high-energy particles. These include electronic devices in satellites subjected to cosmic radiation, and those in nuclear power plants where high-energy reaction products can reach them [1–3]. The damage created by collisions with these particles depends on how they interact with the semiconductor crystals: collisions with nuclei are generally more important at low velocity, while collisions with electrons can dominate at high velocity [4].

Because so many low-velocity particles can be generated at the end of a collision cascade, an important question is as follows: what is the nature of electronic stopping at low velocities? The answer is well known for metallic systems, but much less well understood for insulators. One view has been that, for a material with a gap, there is a threshold velocity v_{th} below which there is no electronic stopping [5–7]. This velocity can be estimated for the case of a channeling atom. If we view it as applying a periodic driving force to the electrons in the semiconductor crystal as it travels down a channel, then the frequency of the driving force is $f = v/\lambda$, where λ is the periodic repeat length of the crystal along the direction the projectile is traveling, and v is the velocity of the channeling atom. The threshold velocity is then given by $v_{\text{th}} = \lambda\Delta/h$, where Δ is the electron energy gap and h is Planck's constant.

Because of the importance of having a proper understanding of the effect of radiation on semiconductors, the stopping of a Si atom by electrons in a silicon crystal was studied recently using time-dependent density-functional theory (TDDFT) [8]. The local density approximation was used for exchange and correlation, so the simulated system had a band gap of about 0.6 eV. For channeling along the [100] direction, the corresponding threshold velocity is 0.2 Å fs^{-1} [8]. We note that a similar value, namely $v'_{\text{th}} = (\frac{2\pi}{3})^{\frac{1}{3}}\lambda\Delta/h$, can be obtained by a different argument based on momentum and energy conservation using a dielectric stopping theory [9]. The main discovery of [8] was that there is significant stopping well below the proposed threshold velocity. This is attributed to a gap state whose energy undulates within the gap as the channeling atom travels through the crystal. As the state approaches the valence band, it is able to collect electronic charge from the filled states. Similarly, as it approaches the conduction band, it is able to deposit charge into the empty conduction states. This process was termed the "electron elevator". This interpretation was supported by simple coupled rate equations that were able to reproduce the variation in the populations of the gap and conduction states [8].

We note that there are similarities between our electron elevator model and the electron promotion model [10,11]. Foremost, they both look at charge transfer by considering the adiabatic states that form when an incident atom or ion interacts with a bulk. However, there is also an important difference, namely the explicit emphasis put on the importance of nonadiabatic processes in our electron elevator model.

The purpose of this paper is to provide a mechanistic description of how the elevator works that can be related directly to the underlying quantum-mechanical description of the electrons. As the adiabatic description of the energy levels in the system provides a good account of most of what is taking place, but cannot account for the small amount of electron transfer to and from the gap state, we choose to use adiabatic perturbation theory (APT) to describe the dynamics of the system [12]. The small quantity in this formalism is the nonadiabatic coupling between states, and it is proportional to the velocity of the channeling atom; thus slow moving atoms correspond to a weak perturbation.

In the next section, we outline the adiabatic perturbation theory formalism that is used [13]. We then summarize the approximations we make to obtain expressions that are

*a.horsfield@imperial.ac.uk

 ©2016 American Physical Society

sufficiently transparent that they can provide insight into how the electron elevator works. Finally, we present numerical results that we can compare with the TDDFT calculations. We find that we can explain much of the TDDFT data with our simplified model.

II. ADIABATIC PERTURBATION THEORY

A. General formulation

Here we present the outlines of the algebra for the perturbation theory. More details about the steps in the argument can be found in the supplemental material [14].

We assume the channeling atom can be treated as a classical particle with a known trajectory $\vec{R}(t)$ inside a crystal. The velocity of the atom is then $\dot{\vec{R}}$, which can vary with time. The electrons respond to the time-varying field the atom applies, with their dynamics being determined by the many-electron Hamiltonian $\hat{H}(\vec{R}(t))$. The evolution of the electrons is then characterized by a many-electron wave function $\Psi(\vec{r},t)$ that satisfies the time-dependent Schrödinger equation $\hat{H}(\vec{R}(t))\Psi(\vec{r},t) = i\hbar\frac{\partial}{\partial t}\Psi(\vec{r},t)$, where $\vec{r}$ represents all the electronic degrees of freedom.

To construct a description of the evolution of the electrons as a perturbation of an adiabatic representation, we require the adiabatic states of the electrons; these are the instantaneous eigenstates $\Phi_n(\vec{R},\vec{r})$, which satisfy the time-independent Schrödinger equation, $\hat{H}(\vec{R})\Phi_n(\vec{R},\vec{r}) = E_n(\vec{R})\Phi_n(\vec{R},\vec{r})$, where $E_n(\vec{R})$ defines a surface of the total energy of the electrons and nuclei, assuming the nuclei are stationary. We now make an expansion for the wave function as

$$\Psi(\vec{r},t) = \sum_n C_n(t)e^{\xi_n(t)/i\hbar}\Phi_n(\vec{R}(t),\vec{r}), \tag{1}$$

where the phase ξ_n is chosen such that the rate of change of the expansion coefficient C_n, namely $\dot{C}_n$, does not depend directly on C_n [hence the omission of the $m = n$ terms in Eq. (3) below]; this allows us to treat large diagonal terms nonperturbatively. In the presence of degeneracies, there can also be large off-diagonal terms; these need a careful treatment that lies beyond the scope of what is presented here. If we substitute our ansatz for the wave function [Eq. (1)] into the time-dependent Schrödinger equation, we find that $\xi_n(t) = \int_0^t [E_n(\vec{R}(s)) + \hbar\gamma_n(\dot{\vec{R}}(s),\vec{R}(s))]ds$ with $\gamma_n(\dot{\vec{R}},\vec{R}) = -i\dot{\vec{R}}\cdot\vec{g}_{nn}(\vec{R})$, where

$$\vec{g}_{nm}(\vec{R}) = \int \Phi_n^*(\vec{R})\vec{\nabla}\Phi_m(\vec{R})d\vec{r}. \tag{2}$$

If the nuclei are taken round a closed path, then the integral of γ_n around the loop is just the well-known Berry phase. Note that for finite systems with real wave functions, $\gamma_n = 0$, a feature we make use of below. The equation of motion for the expansion coefficients is

$$\dot{C}_n(t) = \sum_{m\neq n}\Omega_{nm}(t)C_m(t), \tag{3}$$

where the nonadiabatic coupling rate between surfaces $\Omega_{nm}(t)$ is given by

$$\Omega_{nm}(t) = -e^{i\phi_{nm}(t)}\dot{\vec{R}}(t)\cdot\vec{g}_{nm}(\vec{R}(t)) \tag{4}$$

and

$$\phi_{nm}(t) = \frac{1}{\hbar}\int_0^t [E_n(\vec{R}(s)) - E_m(\vec{R}(s)) + \hbar(\gamma_n(\dot{\vec{R}}(s),\vec{R}(s)) - \gamma_m(\dot{\vec{R}}(s),\vec{R}(s)))]ds. \tag{5}$$

We now seek a perturbative solution to the general equation of motion, Eq. (3). If we assume that the expansion coefficients change little over the duration of the experiment being modeled, then a natural small quantity is the change in the coefficient,

$$\zeta_n(t) = C_n(t) - C_n(0). \tag{6}$$

Restricting the change to be small may at first glance be incompatible with allowing complete electrons to be transferred (say) from the valence band to a defect state in the gap. However, a single electron transition can be thought of as being made up of a series of small transitions of a fraction of an electron. We achieve this below, once we have transformed the many-electron formalism into an independent particle one, by allowing the occupancy of the single-particle defect state to vary. We then have transitions into and out of a partially filled defect state.

If we expand the change as a series of increasing order as

$$\zeta_n = \sum_{p=1}^{\infty}\zeta_n^{(p)} \tag{7}$$

and substitute Eqs. (6) and (7) into Eq. (3), we obtain

$$\sum_{p=1}^{\infty}\dot{\zeta}_n^{(p)}(t) = \sum_{m(\neq n)}\Omega_{nm}(t)C_m(0) + \sum_{m(\neq n)}\Omega_{nm}(t)\sum_{p=1}^{\infty}\zeta_m^{(p)}(t) \tag{8}$$

from which we can make the following identifications:

$$\dot{\zeta}_n^{(1)}(t) = \sum_{m(\neq n)}\Omega_{nm}(t)C_m(0),$$
$$\dot{\zeta}_n^{(p)}(t) = \sum_{m(\neq n)}\Omega_{nm}(t)\zeta_m^{(p-1)}(t) \quad (p > 1). \tag{9}$$

If the system starts in its ground state [$\Psi(\vec{r},0) = \Phi_0(\vec{R},\vec{r})$], then $C_n(0) = \delta_{n,0}$, and the lowest-order expression for the expansion coefficients is

$$C_n(t) = \delta_{n,0} + (1-\delta_{n,0})\int_0^t \Omega_{n0}(s)ds. \tag{10}$$

A quantity we use extensively below is the total excitation energy for the electrons at a given time t. We define this by $\Delta E(t) = \langle\Psi(t)|\hat{H}(\vec{R}(t))|\Psi(t)\rangle - E_0(\vec{R}(t))$, where the angular brackets indicate integration over the electronic degrees of freedom. This can be written in terms of the expansion coefficients to give $\Delta E(t) = \sum_{n>0}|C_n(t)|^2(E_n(\vec{R}(t)) - E_0(\vec{R}(t)))$; as $n = 0$ is the ground state, the sum is over excited states only.

Using the lowest-order expansion of Eq. (10) then gives

$$\Delta E(t) = \sum_{n>0} \left| \int_0^t \Omega_{n0}(s) ds \right|^2 (E_n(\vec{R}(t)) - E_0(\vec{R}(t))). \quad (11)$$

The invariance of this result with respect to the initial phases of the adiabatic states is demonstrated in the Appendix. Note that this result is for many-electron systems. To be able to apply the method to systems with large numbers of electrons, as a practical necessity we reexpress the perturbation theory in an independent electron form in the following section.

B. Simplifying approximations

As we will be comparing our theoretical results with TDDFT simulations, the first natural simplification to make is to replace the full interacting many-body picture of electrons with a noninteracting one. We thus replace the many-particle electronic eigenfunctions with single Slater determinants constructed from molecular orbitals $\phi_i(\vec{R}_i)$ with associated eigenvalues $\epsilon_i(\vec{R}_i)$. In this case, $\vec{g}_{nm}$ is only nonzero if the two Slater determinants differ by just one orbital; this is a result of the way a derivative transforms a product of functions. Thus we can always generate Φ_m from Φ_n by replacing an orbital ϕ_i that is present in Φ_n by an orbital ϕ_j that is not present. Further, as we have formulated the theory so that one of the states is always the ground state, we can replace the index for the other state with the notation $i \to j$ to indicate the change in determinant relative to the ground state: orbital i is removed and replaced by orbital j. Finally, it is also convenient to define the population of the molecular orbital ϕ_i in the ground state to be $f_i \in \{0,1\}$. Applying the above to Eq. (11) then gives

$$\Delta E(t) \approx \sum_{ij} f_i(1-f_j) \left| \int_0^t \Omega_{i\to j,0}(s) ds \right|^2 \times (\epsilon_j(\vec{R}(t)) - \epsilon_i(\vec{R}(t))). \quad (12)$$

To estimate $\Omega_{i\to j,0}$, we first choose the adiabatic eigenstates to be real, so we can set γ_n to zero, as explained above. This allows us to simplify Eq. (5) to

$$\phi_{i\to j,0}(t) = \frac{1}{\hbar} \int_0^t [\epsilon_j(\vec{R}(t)) - \epsilon_i(\vec{R}(t))] ds. \quad (13)$$

If we now assume that the channeling atom travels at constant velocity $\dot{\vec{R}}$ through an infinite crystal, then there will be a fundamental frequency, $\omega = 2\pi|\dot{\vec{R}}|/\lambda$, as discussed in the Introduction. The single-particle eigenvalues $\epsilon_i(\dot{\vec{R}}t)$ will be periodic with this frequency, so the difference $\epsilon_j(\dot{\vec{R}}t) - \epsilon_i(\dot{\vec{R}}t)$ can be written as the sum of a constant part (ϵ_{ij}) and a part $\theta_{ij}(t)$ that is periodic with frequency ω, giving $\epsilon_j(\dot{\vec{R}}t) - \epsilon_i(\dot{\vec{R}}t) = \epsilon_{ij} + \theta_{ij}(t)$. Similarly, the quantity $\dot{\vec{R}} \cdot \vec{g}_{i\to j,0}$ will be periodic with frequency ω, so we can expand the nonadiabatic coupling rate as a Fourier series,

$$\Omega_{i\to j,0}(t) = -\frac{1}{i\hbar} \sum_{l=-\infty}^{\infty} W_{i\to j,l} e^{-i(l\omega - \epsilon_{ij}/\hbar)t}, \quad (14)$$

where the coefficients are given by

$$W_{i\to j,l} = \frac{\omega}{2\pi} \int_{-\pi/\omega}^{\pi/\omega} \exp\left[il\omega t + \frac{i}{\hbar}\int_0^t \theta_{ij}(s) ds \right] \times (\dot{\vec{R}} \cdot i\hbar \vec{g}_{i\to j,0}(\vec{R}(t))) dt. \quad (15)$$

If we substitute Eq. (14) into Eq. (12), take the limit $t \to \infty$, use $\lim_{t\to\infty} t\,\mathrm{sinc}^2(ut) = \pi\delta(u)$, where $\delta(u)$ is the Dirac delta function, and if we neglect the time dependence of $\epsilon_j(\dot{\vec{R}}t) - \epsilon_i(\dot{\vec{R}}t)$ in the energy transfer term (it averages to zero), we obtain the following expression for the stopping power:

$$S = \frac{1}{|\dot{\vec{R}}|} \lim_{t\to\infty} \frac{\Delta E(t)}{t} = \frac{2\pi}{\hbar} \sum_{ij} f_i(1-f_j) \times \sum_{l=-\infty}^{\infty} \frac{l\hbar\omega}{|\dot{\vec{R}}|} |W_{i\to j,l}|^2 \delta(\epsilon_{ij} - l\hbar\omega). \quad (16)$$

We can now see why there need not be a hard threshold at $\Delta = \hbar\omega$. From Eq. (16) we see that transitions are permitted that involve multiples of $\hbar\omega$, allowing damping to occur below the threshold velocity; this is reminiscent of multiphoton ionization by strong fields. If we define $\Gamma_{i\to j,l}$ to be the transition rate from state i to state j due to an excitation of energy $l\hbar\omega$, then we can recast Eq. (16) as $S = \frac{1}{|\dot{\vec{R}}|} \sum_{ij} f_i(1 - f_j) \sum_{l=-\infty}^{\infty} l\hbar\omega \Gamma_{i\to j,l}$, where

$$\Gamma_{i\to j,l} = \frac{2\pi}{\hbar} |W_{i\to j,l}|^2 \delta(\epsilon_{ij} - l\hbar\omega) \quad (17)$$

is the rate at which Fourier component l excites electrons from occupied level i to unoccupied level j.

C. Model matrix elements

To proceed further, we need a model that allows us to estimate $W_{i\to j,l}$. First we assume that the energies of all states are independent of the position of the channeling atom, with the exception of the defect state that appears in the gap, induced by the channeling atom, which varies as

$$\epsilon_d(t) = \bar{\epsilon}_d + \eta\cos(\omega t). \quad (18)$$

This assumption is based on the variation of the energy levels computed in the density-functional theory (DFT) simulations [8]; see Fig. 3. Second, we assume that the adiabatic coupling vector has the form

$$\vec{g}_{i\to j,0} = \frac{\dot{\vec{R}}}{|\dot{\vec{R}}|} \frac{F\sin(\omega t)}{\epsilon_j - \epsilon_i}, \quad (19)$$

where $F\sin(\omega t)$ is a force of amplitude F experienced by the channeling ion. While F is independent of i and j, it has one value for transitions between the valence band and the gap state (F_{vd}), one value for transitions between the conduction band and the gap state (F_{dc}), and one value for transitions between the valence and conduction bands (F_{vc}). The form is motivated by the following identity for the many-electron case:

$$(E_m(\vec{R}) - E_n(\vec{R}))\langle\Phi_m(\vec{R}) \mid \vec{\nabla}\Phi_n(\vec{R})\rangle - \vec{\nabla}E_n(\vec{R})\delta_{nm} = \langle\Phi_m(\vec{R})|\hat{F}(\vec{R})|\Phi_n(\vec{R})\rangle, \quad (20)$$

where $\hat{F}(\vec{R}) = -\vec{\nabla}\hat{H}(\vec{R})$ and the gradient is taken with respect to $\vec{R}$. For the case of direct transitions between the valence and conduction bands, substituting Eq. (19) into Eq. (15) gives

$$W_{v\to c,l} = -\frac{\lambda F_{vc}}{4\pi}[\delta_{l,-1} + \delta_{l,1}], \tag{21}$$

where we have made use of the fact that the valence- and conduction-band energy do not vary with the position of the channeling atom ($\theta_{ij} = 0$), and that $\epsilon_{ij} = l\hbar\omega$ on account of the Dirac δ function in Eq. (16) or Eq. (17). Note that in the presence of a band gap, the $l = 0$ term cannot contribute because of the δ function in Eq. (16), and we just have the $l = \pm 1$ terms. This corresponds to no electronic stopping for channeling atom velocities below our original threshold, so that any stopping below the threshold velocity must be due to the defect state. The absence of any contribution from higher multiples of ω is a consequence of our choice of form for $\vec{g}_{i\to j,0}$ [Eq. (19)]; there could be additional contributions from more sophisticated models, but we expect them to be small.

Let us now consider transitions between the valence or conduction band, and the gap state. Substituting Eqs. (18) and (19) into Eq. (15) gives

$$W_{v\to d,l} = -\frac{\lambda F_{vd}}{4\pi} I_l\left(\frac{\eta}{\hbar\omega}\right), \tag{22}$$

$$W_{d\to c,l} = -\frac{\lambda F_{dc}}{4\pi} I_l\left(-\frac{\eta}{\hbar\omega}\right), \tag{23}$$

where

$$I_l(x) = \frac{2}{\pi}\int_0^{\pi} \frac{\sin(lu + x\sin u)}{l + x\cos u}\sin u\, du. \tag{24}$$

We compute $I_l(x)$ numerically. Note that the integrand can diverge when $|x| \geqslant l$: we manage this by considering the principal part of the integral. The location of the divergence has a physical meaning: it marks when the gap state ceases to be bounded by the valence and conduction bands. To see this, consider the following argument. First, since $\eta = x\hbar\omega$, the condition $|x| < l$ corresponds to $\eta < l\hbar\omega$. Now, for there to be a contribution to the stopping from transitions from the valence band to the defect state, we require $\bar{\epsilon}_d - \bar{\epsilon}_v < l\hbar\omega$, where $\bar{\epsilon}_v$ is the valence-band edge [see Eq. (28) below]. Similarly, for there to be a contribution from transitions from the defect state to the conduction band, we need $\bar{\epsilon}_c - \bar{\epsilon}_d < l\hbar\omega$, where $\bar{\epsilon}_c = \bar{\epsilon}_v + \epsilon_g$ is the conduction-band edge; see Eq. (29) below. If we now observe that η is the amplitude of oscillation of the defect state, we can combine our results to obtain $\eta < \min(\bar{\epsilon}_d - \bar{\epsilon}_v, \bar{\epsilon}_c - \bar{\epsilon}_d)$, which is the result we set out to show. See Fig. 1 for how the integral varies with both the order l and the ratio of η to $\hbar\omega$. The magnitude of the integral decreases with increasing l for a given value of $\eta/\hbar\omega$.

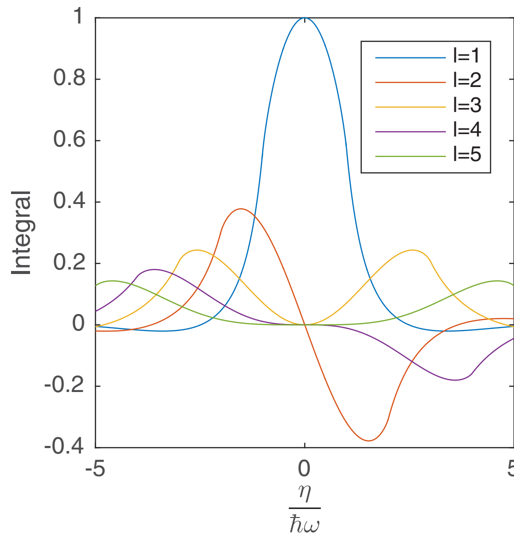

FIG. 1. The variation of the integral I_l with the ratio $\eta/\hbar\omega$ and the order l.

D. Evaluating the sum over states

The ansatz of Eq. (19) means the matrix elements in Eq. (16) depend on the states i and j only through the energies of these states [see Eqs. (21), (22), and (23)]. Thus we can replace the sums over states by integrals over densities of states (DOSs).

For direct transitions between the valence and conduction states, we substitute Eq. (21) into Eq. (16), and we replace the sums over valence and conduction states by an integral over energy weighted by the valence and conduction DOS, D_v and D_c, respectively, giving

$$S_{v\to c} = \frac{\lambda}{2}F_{vc}^2 \int_{\bar{\epsilon}_c}^{\bar{\epsilon}_v + \hbar\omega} D_c(\epsilon_c)D_v(\epsilon_c - \hbar\omega)d\epsilon_c. \tag{25}$$

Note that a factor of 2 for spin degeneracy has been included as the DOS is for a single spin channel only, and we are assuming spin is conserved. In addition, we assume that the population of the valence-band states is always 1, and that of the conduction-band states is always 0. We use the following forms for the densities of states:

$$D_v(\epsilon) = \sum_{i=1}^{4} a_i\sqrt{c_i^2 - (\epsilon - b_i)^2}, \tag{26}$$

$$D_c(\epsilon) = d_c\sqrt{\epsilon - \bar{\epsilon}_c}, \tag{27}$$

where a_i, b_i, and c_i are parameters that are adjusted to give the best fit to the valence-band DOS found from DFT, ϵ_g is the band gap, and d_c is a parameter that is adjusted to give the best fit to the edge of the conduction-band DOS computed from DFT (see Fig. 2). These functional forms are chosen because

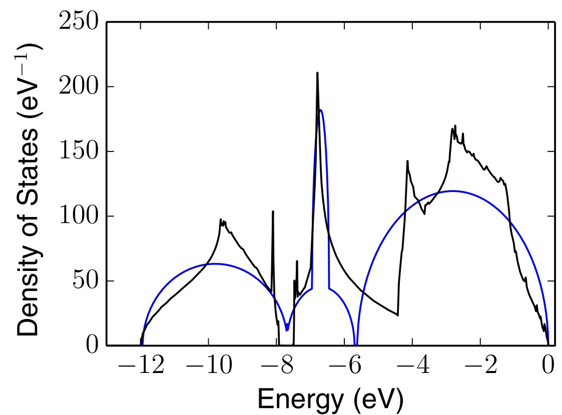

FIG. 2. The valence density of states for Si computed from density-functional theory (black line), and the semielliptical fit used to compute the stopping power (blue line).

TABLE I. The parameters used to describe the channeling of a Si atom in Si.

Parameter	Value
a_1, a_2, a_3, a_4 (eV^{-1})	46.727, 600, 35.525, 50
b_1, b_2, b_3, b_4 (eV)	−2.808, −6.7, −9.8, −6.7
c_1, c_2, c_3, c_4 (eV)	−2.808, −0.25, −2.136, −1.0
d_c (eV$^{-\frac{3}{2}}$)	43.2
F_{vd}, F_{dc}, F_{cv} (eV Å^{-1})	0.168, 0.119, 0.009
η (eV)	0.1
$\bar{\epsilon}_d - \bar{\epsilon}_v$ (eV)	0.26
ϵ_g (eV)	0.5
λ (Å)	1.353 225

they reproduce the correct shape of the band edges. See Table I for the values of the parameters used.

Starting from Eq. (16), and substituting in Eqs. (22) and (23) for the contribution to the stopping from transitions from the valence band to the gap state, we get

$$S_{v\to d} = \frac{\lambda}{2}F_{vd}^2(1-f_d)\sum_{l=-\infty}^{\infty} l\left|I_l\left(\frac{\eta}{\hbar\omega}\right)\right|^2 D_v(\bar{\epsilon}_d - l\hbar\omega), \tag{28}$$

while that from transitions from the gap state to the conduction band is given by

$$S_{d\to c} = \frac{\lambda}{2}F_{dc}^2 f_d\sum_{l=-\infty}^{\infty} l\left|I_l\left(\frac{-\eta}{\hbar\omega}\right)\right|^2 D_c(\bar{\epsilon}_d + l\hbar\omega), \tag{29}$$

where $0 \leqslant f_d \leqslant 1$ is the population of the gap state per spin.

The total stopping S is given by a sum over the three contributions enumerated above: $S = S_{v\to c} + S_{v\to d} + S_{d\to c}$.

E. The population of the defect state

The contributions to the stopping power that involve the defect state require the steady-state population f_d. This can be computed directly from the net transition rates to and from the defect state. Once the steady state has been reached, to hold the population of the defect state fixed, the number of electrons moving from the valence band to the defect state must exactly equal the number moving from the defect state to the conduction band. If we introduce the rates $\Gamma_{v\to d}$ and $\Gamma_{d\to c}$ for transitions of electrons of a given spin from the valence band to the gap state, and for the gap state to the conduction band, respectively, we have $2(1-f_d)\Gamma_{v\to d} = 2f_d\Gamma_{d\to c}$. We can rearrange this to obtain f_d

$$f_d = \frac{\Gamma_{v\to d}}{\Gamma_{v\to d} + \Gamma_{d\to c}}. \tag{30}$$

We can obtain the relevant rates from Eq. (17). After introducing the relevant DOS and matrix elements [Eqs. (22) and (23)], we obtain

$$\Gamma_{v\to d} = \frac{2\pi}{\hbar}\left|\frac{\lambda F_{vd}}{4\pi}\right|^2 \sum_{l=-\infty}^{\infty}\left|I_l\left(\frac{\eta}{\hbar\omega}\right)\right|^2 D_v(\bar{\epsilon}_d - l\hbar\omega) \tag{31}$$

and

$$\Gamma_{d\to c} = \frac{2\pi}{\hbar}\left|\frac{\lambda F_{dc}}{4\pi}\right|^2 \sum_{l=-\infty}^{\infty}\left|I_l\left(\frac{-\eta}{\hbar\omega}\right)\right|^2 D_c(\bar{\epsilon}_d + l\hbar\omega). \tag{32}$$

In passing, we also note that the rate of direct transitions between the valence and conduction bands is

$$\Gamma_{v\to c} = \frac{2\pi}{\hbar}\left|\frac{\lambda F_{vc}}{4\pi}\right|^2 \int_{\bar{\epsilon}_v+\epsilon_g}^{\infty} D_c(\epsilon_c)D_v(\epsilon_c - \hbar\omega)d\epsilon_c. \tag{33}$$

F. Estimating the parameters

We now estimate the values of the quantities required by our model. All values can be found in Table I.

As for the DOS parameters discussed above, the band gap (ϵ_g), valence-band edge ($\bar{\epsilon}_v$), and gap state parameters ($\bar{\epsilon}_d$ and η) can be obtained readily from DFT simulations; see Fig. 3. Similarly, once we know the structure of our crystal, and the speed and direction of the channeling atom, we can obtain λ, v, and ω. That leaves the force magnitudes F_{vd}, F_{dc}, and F_{cv}.

At larger channeling velocities ($\hbar\omega > \epsilon_g$), the electronic stopping is dominated by direct transitions from the valence band to the conduction band because of the large number of states available, and thus we have $S \approx S_{v\to c}$. The high-velocity regime corresponds to the linear region in Fig. 4. The force magnitude F_{vc} can thus be obtained by equating the right-hand side of Eq. (25) with the total stopping obtained from TDDFT simulations, giving

$$F_{vc} = \sqrt{\frac{2S}{\lambda\int D_c(\epsilon_c)D_v(\epsilon_c - \hbar\omega)d\epsilon_c}}. \tag{34}$$

At intermediate channeling velocities [$\min(\bar{\epsilon}_d - \bar{\epsilon}_v, \epsilon_g - (\bar{\epsilon}_d - \bar{\epsilon}_v)) < \hbar\omega < \epsilon_g$], the stopping is dominated by transitions involving the gap state, as was shown in Ref. [8]. As these transitions are dominated by the $l = 1$ contribution (see Fig. 4), the steady-state condition $2(1-f_d)\Gamma_{v\to d} = 2f_d\Gamma_{d\to c}$ leads directly to $S_{v\to d} = S_{d\to c}$. Further, since direct transitions

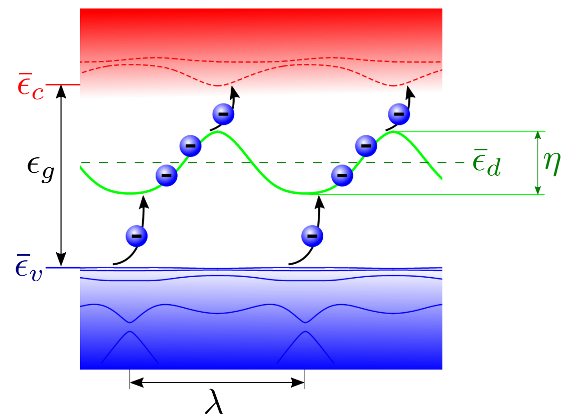

FIG. 3. This figure shows how the gap state can operate as an elevator that transfers an electron from the valence band to the conduction band. The horizontal position corresponds to the location of the channeling atom. The blue, green, and red areas show that the energies of the states in the valence band, the gap, and the conduction band, respectively, vary with the location of the channeling atom. The states are adiabatic.

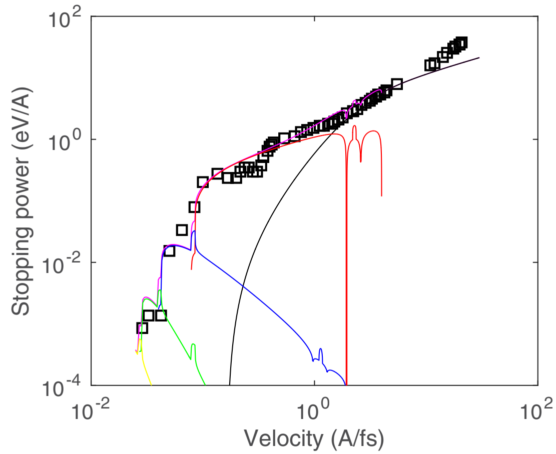

FIG. 4. The breakdown into components of the stopping of the Si atom channeling along the (001) direction in Si. The black squares are the results from the TDDFT simulations. The magenta line is the total stopping computed from perturbation theory (PT). The solid black line corresponds to the PT stopping power from direct transitions from the valence to the conduction bands. The red, blue, green, and yellow lines correspond to the PT stopping powers mediated by the defect state for $l = 1,2,3$, and 4, respectively. Note that the excitation energy ($\hbar\omega$) can be found from the velocity (v) using $\hbar\omega/\mathrm{eV} = 3.056v/(\text{Å}\ \ \mathrm{fs}^{-1})$, where we have used $\omega = \frac{2\pi v}{\lambda}$ and the value of λ from Table I.

between the valence and conduction bands are not important in this regime, we can write $S \approx 2S_{v\to d} = 2S_{d\to c}$. Thus, using the stopping power S from a TDDFT simulation together with Eqs. (28) and (29), keeping $l = 1$ only, we obtain

$$F_{vd} = \frac{1}{\left|I_1\left(\frac{\eta}{\hbar\omega}\right)\right|}\sqrt{\frac{S}{\lambda(1-f_d)D_v(\bar{\epsilon}_d - \hbar\omega)}} \tag{35}$$

and

$$F_{dc} = \frac{1}{\left|I_1\left(-\frac{\eta}{\hbar\omega}\right)\right|}\sqrt{\frac{S}{\lambda f_e D_c(\epsilon_d + \hbar\omega)}}. \tag{36}$$

III. RESULTS

Having developed a model for the operation of the electron elevator, as well as direct transitions across the band gap, we now use it to interpret the electronic stopping computed for a Si channeling along the (001) direction in a Si crystal computed using TDDFT [8]. The main results are shown in Fig. 4.

First we note that the agreement between the results for the total stopping from TDDFT and PT is very good, except at the highest velocities. The high-velocity errors originate with the rather simple approximation we make for the conduction-band DOS; the approximation is, however, adequate for our primary task of understanding the low-velocity regime.

The direct transitions from valence to conduction band make a smooth contribution that only becomes important once $\hbar\omega$ is of the same size as the band gap (0.6 eV). This is what we might expect based on the argument that the channeling ion imposes an oscillating field on the electrons in the crystal. For transitions involving the defect state, with $l = 1$ we find a fairly uniform contribution (modulated by the valence DOS) over an energy range corresponding to the width of the valence band. This again can be understood as originating from the oscillating field, but now the electrons need to be excited from the valence band into the defect state. The $l = 2$ contribution spans about half the energy range of the $l = 1$ case, as expected, but it also drops off faster with increasing velocity. The drop off is a result of the shape of the integral I_2, which falls away roughly linearly with $1/v$ (see Fig. 1). It also is significant at velocities below those at which $l = 1$ is important. This separation of the contributions to stopping from individual values of l continues at lower velocity for $l = 3$ and 4. The separation is due to the form of the integrals I_3 and I_4 (see Fig. 1).

An important contributor to the stopping involving the defect state is the population of that state. This is presented as a function of channeling ion velocity in Fig. 5. The shape again tracks the valence DOS, as might be expected from Eqs. (30), (31), and (32). However, there are additional reductions in the occupation at lower velocity over narrow velocity windows: these are a result of the form of the integrals I_l: they drop off quickly when $\hbar\omega$ is outside the range $\eta/(l-1) < \hbar\omega < \eta/l$ (see Fig. 1).

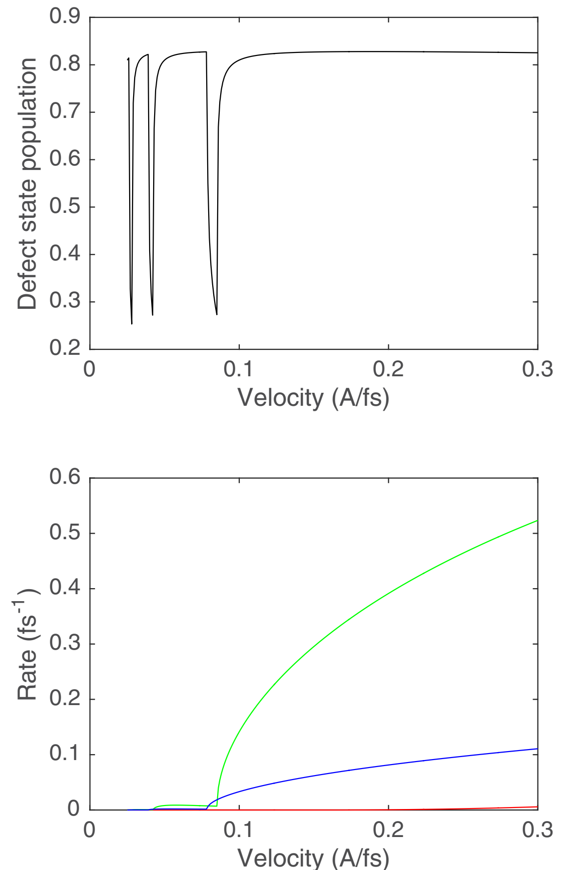

FIG. 5. Upper panel: population of the defect state as a function of velocity of the channeling atom, computed from perturbation theory. The structure follows that of the valence density of states, with additional structure at low velocity from the integral I_l. Lower panel: the transition rates between valence and conduction bands (red), the valence band and the defect state (green), and the defect state and the conduction band (blue).

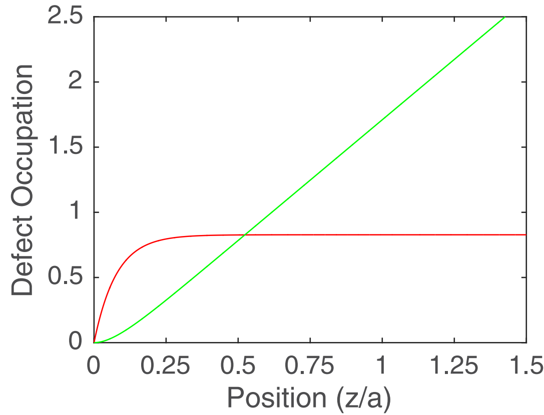

FIG. 6. The occupation of the defect state (red) and conduction band (green) as a function of channeling atom position for an atom moving at 0.164 Å fs^{-1}.

The defect population is related to the transition rates [see Eq. (30)]. These rates are plotted in Fig. 5; note that the plotted rates include a factor of 2 for spin degeneracy. The rates are not the same as those reported in [8]; in particular, the transition rate between the valence band and the defect state is much larger than that between the defect state and the conduction band (the reverse of what is reported in [8]). Given that both sets of results were obtained by fitting to the same data, it suggests that there is some flexibility in the fitting.

In Fig. 6, we have plotted the defect state and conduction-band populations as a function of channeling atom position using the rate equations from [8], but using the rates computed using perturbation theory. While not identical with the reported curves, they are qualitatively similar; in particular, they reproduce the steplike features in the limit $v \to 0$ [15].

IV. CONCLUSION

Recently, we demonstrated, by means of TDDFT simulations, that electron stopping of channeling atoms can occur even when the velocity is too low for direct excitation of electrons across the band gap [8]. We argued that this is because the channeling atom creates a defect state in the band gap that is able to pick up an electron from the valence band and carry across the gap to the conduction band, a mechanism we titled the electron elevator. Here we use a simple model derived from adiabatic perturbation theory to give a more detailed account of how the elevator operates. A key finding is that electrons experience a perturbation that oscillates in time not only at the repeat frequency f of the channeling atom, but also at multiples of this frequency, characterized by the integer order l. The larger the value of l, the lower the velocity of the channeling atom needs to be to induce electronic excitations. In the case of Si channeling in Si, for the transitions that occur by means of the defect state, the contribution drops off rapidly with increasing l, but it remains significant up to $l = 4$. For other systems, the number of significant values of l could be different. For direct transitions across the band gap, only $l = 1$ contributes.

ACKNOWLEDGMENTS

A.L. was supported by the CDT in Theory and Simulation of Materials at Imperial College London funded by EPSRC Grant No. EP/G036888/1 and the Thomas Young Centre under Grant No. TYC-101. Work by A.A.C. was performed under the auspices of the U.S. Department of Energy by Lawrence Livermore National Laboratory under Contract No. DE-AC52-07NA27344.

APPENDIX: GAUGE INVARIANCE OF THE STOPPING POWER

The choice of phase for the eigenstates is arbitrary; here we show that the final result is independent of this choice. Consider two families of solutions $\Phi_n(\vec{R})$ and $\tilde{\Phi}_n(\vec{R}) = e^{i\chi_n(\vec{R})}\Phi_n(\vec{R})$. Setting $\vec{v}(t) = \dot{\vec{R}}(t)$, the corresponding expectation values of the gradient operator are

$$\gamma_n(t) = -i\vec{v}(t)\cdot\int \Phi_n^*(\vec{R}(t))\vec{\nabla}\Phi_n(\vec{R}(t))d\vec{r}, \tag{A1}$$

$$\tilde{\gamma}_n(t) = \gamma_n(t) + \vec{v}(t)\cdot\vec{\nabla}\chi_n(\vec{R}). \tag{A2}$$

The corresponding wave-function expansions [see Eq. (1)] are

$$\Psi(t) = \sum_n C_n(t)\exp\left(\frac{1}{i\hbar}\int_0^t [E_n(\vec{R}(s)) + \hbar\gamma_n(s)]ds\right) \times \Phi_n(\vec{R}(t)), \tag{A3}$$

$$\tilde{\Psi}(t) = \sum_n \tilde{C}_n(t)e^{i\chi_n(\vec{R}(t))}\exp\left(\frac{1}{i\hbar}\int_0^t [E_n(\vec{R}(s)) + \hbar\gamma_n(s) + \hbar\vec{v}(t)\cdot\vec{\nabla}\chi_n(\vec{R})]ds\right)\Phi_n(\vec{R}(t)). \tag{A4}$$

Now $\vec{v}(t)\cdot\vec{\nabla}\chi_n(\vec{R}(t)) = \frac{\partial}{\partial t}\chi_n$, so that $\exp(\frac{1}{i\hbar}\int_0^t[\hbar\vec{v}(t)\cdot\vec{\nabla}\chi_n(\vec{R})]ds) = \exp(-i[\chi_n(\vec{R}(t)) - \chi_n(\vec{R}(0))])$. Substituting into Eq. (A4) gives

$$\tilde{\Psi}(t) = \sum_n \tilde{C}_n(t)e^{i\chi_n(\vec{R}(0))}\exp\left(\frac{1}{i\hbar}\int_0^t [E_n(\vec{R}(s)) + \hbar\gamma_n(s)]ds\right)\Phi_n(\vec{R}(t)). \tag{A5}$$

Comparing Eqs. (A3) and (A5), we see that $\Psi(t) = \tilde{\Psi}(t)$ provided $\tilde{C}_n(t)e^{i\chi_n(\vec{R}(0))} = C_n(t)$. That is, the coefficients differ only by a constant phase, which will have no effect on our primary result, Eq. (11).

[1] J. Baur, B. Engholm, M. Hacker, I. Maya, P. Miller, W. Toffolo, and S. Wojtowicz, Radiation hardening of diagnostics for fusion reactors (Office of Scientific and Technical Information, Oak Ridge, TN, 1981).

[2] P. Stott, Diagnostics for Experimental Thermonuclear Fusion Reactors, in *Proceedings of the International School of Plasma Physics "Piero Caldirola," Workshop on Diagnostics for Experimental Fusion Reactors: Varenna, Italy*, (Plenum, NY, 1998).
[3] *Radiation Hardness Assurance for Space Systems*, edited by C. Poivey (IEEE, Piscataway, NJ, 2002).
[4] J. Ziegler, M. Ziegler, and J. Biersack, Nucl. Instrum. Methods Phys. Res., Sect. B **268**, 1818 (2010).
[5] J. M. Pruneda, D. Sánchez-Portal, A. Arnau, J. I. Juaristi, and E. Artacho, Phys. Rev. Lett. **99**, 235501 (2007).
[6] S. N. Markin, D. Primetzhofer, and P. Bauer, Phys. Rev. Lett. **103**, 113201 (2009).
[7] F. Mao, C. Zhang, J. Dai, and F.-S. Zhang, Phys. Rev. A **89**, 022707 (2014).
[8] A. Lim, W. M. C. Foulkes, A. P. Horsfield, D. R. Mason, A. Schleife, E. W. Draeger, and A. A. Correa, Phys. Rev. Lett. **116**, 043201 (2016).
[9] Z. H. Levine and S. G. Louie, Phys. Rev. B **25**, 6310 (1982).
[10] U. Fano and W. Lichten, Phys. Rev. Lett. **14**, 627 (1965).
[11] R. Souda, T. Suzuki, and K. Yamamoto, Surf. Sci. **397**, 63 (1998).
[12] A. M. L. Messiah, *Quantum Mechanics* (North-Holland, Amsterdam, 1962).
[13] A. Lim, Ph.D. thesis, Imperial College, 2014.
[14] See supplemental material at http://link.aps.org/supplemental/10.1103/PhysRevB.93.245106 for an expanded version of the perturbation theory algebra.
[15] E. Artacho, J. Phys.: Condens. Matter **19**, 275211 (2007).